AIMS Mathematics, 10(3): 5859–5879.
DOI: 10.3934/math.2025269
Received: 09 January 2025
Revised: 27 February 2025
Accepted: 04 March 2025
Published: 17 March 2025

https://www.aimspress.com/journal/Math

Research article

Stochastic solutions of the geophysical KdV equation: Numerical simulations and white noise impact

Areej A. Almoneef[1], Abd-Allah Hyder[2,*], Mohamed A. Barakat[3] and Abdelrheem M. Aly[2]

[1] Department of Mathematical Sciences, College of Science, Princess Nourah Bint Abdulrahman University, P.O. Box 84428, Riyadh 11671, Saudi Arabia

[2] Department of Mathematics, College of Science, King Khalid University, Box 9004, 61413, Abha, Saudi Arabia

[3] Department of Basic Science, University College of Alwajh, University of Tabuk, Saudi Arabia

* **Correspondence:** Email: abahahmed@kku.edu.sa.

Abstract: This research explored stochastic soliton and periodic wave (SPW) solutions for the geophysical Korteweg-de Vries (KdV) equation with variable coefficients, incorporating the effects of Earth's rotation, fluid stratification, and topographical variations. The classical KdV equation, widely used to model nonlinear wave propagation, was extended to describe geophysical wave dynamics in atmospheric and oceanic systems. Exact solutions for both the deterministic and Wick-type stochastic (W-TS) forms of the geophysical KdV equation were obtained using white noise (WN) theory, the Hermite transform (HT), and the exp-function method. By employing the HT, the stochastic equation was transformed into a deterministic counterpart, facilitating the derivation of novel SPW solutions expressed as rational functions involving exponential terms. The inverse HT is then applied to retrieve stochastic SPW solutions under Gaussian WN conditions. Numerical analysis highlights the influence of Brownian motion (B-M) on the formation and behavior of SPWs in geophysical settings. Additionally, numerical simulations illustrate how random fluctuations affect wave stability and evolution, offering deeper insights into nonlinear wave interactions in oceanic and atmospheric environments.

Keywords: geophysical KdV equation; soliton and periodic wave solutions; white noise effects; exp-function method; numerical simulations
Mathematics Subject Classification: 35Q53, 60H15, 37K40

1. Introduction

Nonlinear partial differential equations (PDEs) arise from the mathematical modeling of complex physical systems. Investigating these nonlinear physical models through the analysis of their wave solutions plays a crucial role in applied sciences. The Korteweg-de Vries (KdV) equations, in particular, serve as models for nonlinear wave propagation across a wide range of material science applications. Initially developed to describe long-wavelength, small-amplitude shallow water waves, the KdV equation has proven useful in numerous physical scenarios. Its soliton and periodic exact solutions are relevant to phenomena such as collisionless hydromagnetic waves, internal stratified waves, particle acoustic waves, and plasma dynamics. For more details, see references [1–5]. In geophysical fluid dynamics, the KdV equation is extended to account for more complex phenomena relevant to large-scale waves in the atmosphere and ocean. These geophysical KdV equations incorporate the effects of Coriolis forces (due to Earth's rotation), stratification (layering of fluids with different densities), and variable topography (changing ocean depth), making them crucial for understanding wave propagation in natural environments [6–9]. For example, the KdV equation is used to model shallow water waves and internal waves in the ocean, as well as atmospheric gravity waves. Internal waves, which occur in stratified fluids like the ocean, propagate along interfaces between layers of different densities and are essential for mixing and energy transfer in the ocean [10, 11]. In [12], internal solitons have been observed and simulated, particularly in areas like the South China Sea, confirming the accuracy of KdV-based models in practical environments. The rotational KdV equation incorporates Earth's rotational effects and has been employed to examine equatorial waves and other large-scale wave patterns [13]. Different forms of the KdV equation, including the variable-coefficient KdV and the KdV-Burgers equation (which accounts for dissipative processes), are utilized to represent wave behavior over varying depths and under conditions involving damping, see [14, 15]. The geophysical KdV equations provide a robust framework for understanding nonlinear wave dynamics in both oceanographic and atmospheric contexts. These equations offer insight into a wide range of phenomena, from coastal wave propagation to the behavior of atmospheric disturbances, making them a key tool in geophysical fluid dynamics, see [16–18].

This work is devoted to investigating the stochastic geophysical KdV equation:

$$\frac{\partial}{\partial \nu}Z(\mu,\nu)+\Psi(\nu)\diamond\frac{\partial}{\partial \mu}Z(\mu,\nu)+\Phi(\nu)\diamond Z(\mu,\nu)\diamond\frac{\partial}{\partial \mu}Z(\mu,\nu)+\Xi(\nu)\diamond\frac{\partial^3}{\partial \mu^3}Z(\mu,\nu)=0, \tag{1.1}$$

where $(\mu,\nu)\in\mathbb{R}\times\mathbb{R}_+$ and Ψ, Φ, and Ξ are non-zero integrable functions from $\mathbb{R}^+$ to the Kondrative distribution space $(\mathcal{T})_{-1}$ which was defined by Holden et al. in [20] as a Banach algebra with the Wick-product "$\diamond$". Equation (1.1) is the perturbation of the variable coefficients geophysical KdV equation:

$$\frac{\partial}{\partial \nu}z(\mu,\nu)+\psi(\nu)\frac{\partial}{\partial \mu}z(\mu,\nu)+\phi(\nu)z(\mu,\nu)\frac{\partial}{\partial \mu}z(\mu,\nu)+\xi(\nu)\frac{\partial^3}{\partial \mu^3}z(\mu,\nu)=0. \tag{1.2}$$

The geophysical KdV equation (1.2) represents an extension of the classical KdV equation, adjusted to describe wave phenomena in geophysical contexts, such as the oceans and atmosphere. This formulation takes into account the Coriolis effect, which models the deflection due to the Earth's rotation [19]. In Eq (1.2), the term ψ represents the Coriolis effect, which is responsible for the deflection of objects in motion, such as air or water, caused by the Earth's rotation. The coefficient

ϕ captures the nonlinearity, while ξ characterizes the dispersion, illustrating how a complex wave breaks down into its component wavelengths. Additionally, if Eq (1.2) is studied in a stochastic framework, it leads to the stochastic version of the geophysical KdV equation. In this case, the functions Ψ, Φ, and Ξ serve as the stochastic counterparts of ψ, ϕ, and ξ, respectively, thereby accounting for random perturbations within the geophysical wave system. To obtain precise solutions to this stochastic geophysical KdV equation, we confine our analysis to a WN setting, which leads us to the W-TS geophysical KdV equation (1.1). Recent studies have integrated both numerical and analytical approaches to further understand the dynamics of the KdV equation.

In recent years, a significant number of studies have focused on partial differential equations (PDEs) and the exact solutions of such equations using various methodologies. In [21], the first integral method was applied to determine exact solutions for nonlinear PDEs involving the beta-derivative. Moreover, solutions in the form of optical, dark, complex, and singular solitons have been found for certain nonlinear PDEs using the M-derivative approach [22, 23]. The examination of exact and approximate solutions for nonlinear evolution equations is essential for comprehending nonlinear physical phenomena. Several efficacious methodologies have been suggested, including the bilinear transformation method [24], the modified Clarkson and Kruskal (CK) direct method [25], the multiscale expansion approach [26], the binary Bell polynomials technique [27], the Riemann-Hilbert method [28], and the approximate symmetry method [29]. The exp-function method, presented by He and Wu [30], offers a direct approach for deriving generalized soliton, periodic, and compacton-like solutions for several nonlinear partial differential equations. This approach expresses solutions as rational functions of the exponential form, with both the numerator and denominator being polynomials of exponential functions. The primary benefit of the exp-function method is its capacity to produce a diverse array of exact solutions for nonlinear partial differential equations by varying parameters and polynomial degrees in the solutions. A fundamental characteristic of solutions derived from this method is their reducibility [31]. Furthermore, the exp-function method produces both generalized soliton and periodic solutions. The procedure is streamlined through the utilization of Mathematica and can be efficiently implemented for many nonlinear equations. Recent studies have further explored the KdV equation using the exp-function method, providing new perspectives on soliton and periodic wave solutions. For instance, recent work [32] has investigated these techniques in depth, which reinforces the relevance of our approach in addressing stochastic influences in geophysical settings. Modern studies have examined the strain wave equation in micro-structured solids, deriving various analytical solutions through advanced mathematical methods [33].

While existing studies, such as Zhang [34], have investigated exact solutions for Wick-type stochastic KdV equations, this paper presents several key advancements. We derive new stochastic SPW solutions for the variable coefficient geophysical KdV equation and the W-TS geophysical KdV equation. Through the use of WN theory and the HT, the W-TS geophysical KdV equation is converted into its deterministic counterpart. By applying the exp-function method, we construct exact solutions for the deterministic geophysical KdV equation, represented as an exponential-type rational function, with polynomials of exponential functions in both the numerator and denominator. The highest-order linear term and the highest-order nonlinear term of the deterministic geophysical KdV equation are balanced to determine the polynomial degrees in both parts. With symbolic computation in Mathematica, SPW solutions for the variable coefficient geophysical KdV equation are found. Under certain conditions, we apply the inverse HT to extract stochastic SPW solutions for the W-

TS geophysical KdV equation. Additionally, an example with numerical simulations is presented to analyze the impact of Gaussian WN on SPW dynamics, providing deeper insight into how random perturbations influence wave behavior.

The structure of the paper is as follows: Section 2 reviews key definitions and properties relevant to Gaussian WN analysis and outlines the primary steps in solving nonlinear PDEs. In Section 3, we use the exp-function method, WN theory, and the HT to derive deterministic solutions for the W-TS geophysical KdV equation. Section 4 applies the inverse HT to obtain stochastic SPW solutions for the W-TS geophysical KdV equation. In Section 5, we provide an example with numerical simulations, demonstrating that stochastic solutions can be expressed as B-M functionals. Finally, Section 6 concludes with a summary of the results and findings.

2. Fundamental concepts of the white noise framework

The foundational study of WN structure begins with the inclusion chain $\mathcal{T}(\mathbb{R}^n) \subset L^2(\mathbb{R}^n) \subset \mathcal{T}^\star(\mathbb{R}^n)$. Here, $\mathcal{T}(\mathbb{R}^n)$ denotes the space of test functions, which are infinitely differentiable and rapidly vanishing on $\mathbb{R}^n$, while $\mathcal{T}^\star(\mathbb{R}^n)$ refers to the space of tempered distributions. By the Bochner-Minlos theorem [20], there exists a unique WN measure ν on $(\mathcal{T}^\star(\mathbb{R}^n), \theta(\mathcal{T}^\star(\mathbb{R}^n)))$.

Consider the Hermite functions $\zeta_m(x) = \pi^{-1/4}((m-1)!)^{-1/2}e^{-x^2/2}p_{m-1}(\sqrt{2}x)$ for $m \in \mathbb{N}$, where $p_m(x)$ are Hermite polynomials. It is well known that the family $\{\zeta_m\}_{m\in\mathbb{N}}$ forms an orthonormal basis for $L^2(\mathbb{R})$. Let $\beta = (\beta_1, \ldots, \beta_n)$ represent a multi-index of dimension n, where $\beta_1, \ldots, \beta_n \in \mathbb{N}$. The tensor product family $\zeta_\beta := \zeta_{(\beta_1,\ldots,\beta_n)} = \zeta_{\beta_1} \otimes \cdots \otimes \zeta_{\beta_n}$, $\beta \in \mathbb{N}^n$, serves as an orthonormal basis for $L^2(\mathbb{R}^n)$. To further proceed, we establish an ordering on $\mathbb{N}^n$ as follows:

$$r < s \Rightarrow \sum_{j=1}^{n} \beta_j^{(r)} \leq \sum_{j=1}^{n} \beta_j^{(s)}, \quad \text{where} \quad \beta^{(r)} = (\beta_j^{(r)})_{j=1}^n,\ \beta^{(s)} = (\beta_j^{(s)})_{j=1}^n \in \mathbb{N}^n.$$

Using this ordering, define $\kappa_r := \zeta_{\beta^{(r)}} = \zeta_{\beta_1^{(r)}} \otimes \cdots \otimes \zeta_{\beta_n^{(r)}}$, $r \in \mathbb{N}$. Let $\mathbb{K} = \left(\mathbb{N}_0^{\mathbb{N}}\right)_c$ denote the set of sequences $\beta = (\beta_i)_{i\in\mathbb{N}}$ where $\beta_i \in \mathbb{N}_0$ and has compact support. For $\beta \in \mathbb{K}$, define

$$\mathcal{H}_\beta(\omega) = \prod_{i=1}^{\infty} p_{\beta_i}(\langle \omega, \kappa_i \rangle), \quad \omega \in \mathcal{T}^\star(\mathbb{R}^n).$$

Let $m \in \mathbb{N}$, the Kondratiev space of stochastic test functions $(\mathcal{T})_1^m$ is defined as:

$$(\mathcal{T})_1^m = \left(f = \sum_\beta d_\beta \mathcal{H}_\beta \in \bigoplus_{j=1}^{m} L^2(\nu) :\ d_\beta \in \mathbb{R}^m \text{ and } \|f\|_{1,j}^2 := \sum_\beta d_\beta^2 (\beta!)^2 (2\mathbb{N})^{j\beta} < \infty,\ \forall\, j \in \mathbb{N} \right),$$

and the Kondratiev space of stochastic distributions $(\mathcal{T})_{-1}^m$ is defined as:

$$(\mathcal{T})_{-1}^m = \left(F = \sum_\beta e_\beta \mathcal{H}_\beta :\ e_\beta \in \mathbb{R}^m \text{ and } \|F\|_{-1,j}^2 := \sum_\beta e_\beta^2 (2\mathbb{N})^{-p\beta} < \infty \text{ for some } p \in \mathbb{N} \right).$$

The family of seminorms $\|f\|_{1,j}$, $j \in \mathbb{N}$, induces a topology on $(\mathcal{T})_1^m$, and $(\mathcal{T})_{-1}^m$ is the dual space of $(\mathcal{T})_1^m$ with the pairing

$$\langle F, f \rangle = \sum_\beta (e_\beta, d_\beta)\beta!,$$

where $F = \sum_\beta e_\beta \mathcal{H}_\beta \in (\mathcal{T})^m_{-1}$, $f = \sum_\beta d_\beta \mathcal{H}_\beta \in (\mathcal{T})^m_1$, and (e_β, d_β) represents the usual scalar product in $\mathbb{R}^m$.

The Wick product of two distributions $F = \sum_\beta u_\beta \mathcal{H}_\beta$, $G = \sum_\gamma v_\gamma \mathcal{H}_\gamma \in (\mathcal{T})^m_{-1}$ with $u_\beta, v_\gamma \in \mathbb{R}^m$ is defined by:

$$F \diamond G = \sum_{\beta,\gamma} (u_\beta, v_\gamma) \mathcal{H}_{\beta+\gamma}.$$

Let $F = \sum_\beta u_\beta \mathcal{H}_\beta \in (\mathcal{T})^m_{-1}$ with $u_\beta \in \mathbb{R}^m$. The HT of F is defined as:

$$\mathcal{G}F(w) = \widetilde{F}(w) = \sum_\beta u_\beta w^\beta \in \mathbb{C}^m \quad \text{(when convergent)},$$

where $w = (w_1, w_2, \dots) \in \mathbb{C}^{\mathbb{N}}$ and $w^\beta = \prod_{i=1}^\infty w_i^{\beta_i}$, with $\beta = (\beta_1, \beta_2, \dots) \in \mathbb{K}$ and $w_i^0 = 1$.

For $F, G \in (\mathcal{T})^m_{-1}$, the HT gives:

$$\widetilde{F \diamond G}(w) = \widetilde{F}(w)\widetilde{G}(w),$$

for all w where $\widetilde{F}(w)$ and $\widetilde{G}(w)$ are defined. The multiplication on the right-hand side corresponds to the standard bilinear multiplication in $\mathbb{C}^m$, defined by $(w_1^1, \dots, w_m^1) \cdot (w_1^2, \dots, w_m^2) = \sum_{i=1}^m w_i^1 w_i^2$, where $w_i^k \in \mathbb{C}$. Consequently, the HT translates the Wick product into regular multiplication, and convergence in $(\mathcal{T})^m_{-1}$ is equivalent to pointwise convergence within a neighborhood of zero in $\mathbb{C}^m$. For additional details on Kondratiev spaces, the Wick product, and the HT, please refer to [20].

One of the most important tools for obtaining our conclusions is the following theorem.

Theorem 2.1. *[20] Let $z(\mu, \nu, w)$ be a solution to the following equation:*

$$\widetilde{\Omega}(\mu, \nu, \frac{\partial}{\partial \nu}, \frac{\partial}{\partial \mu_1}, \dots, \frac{\partial}{\partial \mu_n}, z, w) = 0, \tag{2.1}$$

for (μ, ν) in some bounded open region $\mathbb{O} \subset \mathbb{R}^n \times \mathbb{R}_+$, and for all $w \in \mathcal{N}_\alpha(u)$, for some $\alpha < \infty, u > 0$. Further assume that $z(\mu, \nu, w)$, along with all of its derivatives involved in (2.1)*, are uniformly bounded for $(\mu, \nu, w) \in \mathbb{O} \times \mathcal{N}_\alpha(u)$, continuous with respect to $(\mu, \nu) \in \mathbb{O}$ for each $w \in \mathcal{N}_\alpha(u)$, and analytic in $w \in \mathcal{N}_\alpha(u)$ for all $(\mu, \nu) \in \mathbb{O}$. Then there exists a stochastic distribution $Z(\mu, \nu) \in (\mathcal{T})_{-1}$ such that $z(\mu, \nu, w) = \widetilde{Z}(\mu, \nu)(w)$ for all $(\mu, \nu, w) \in \mathbb{O} \times \mathcal{N}_\alpha(u)$, and $Z(\mu, \nu)$ satisfies the equation:*

$$\Omega^\diamond(\mu, \nu, \frac{\partial}{\partial \nu}, \frac{\partial}{\partial \mu_1}, \dots, \frac{\partial}{\partial \mu_n}, Z) = 0, \tag{2.2}$$

in the strong sense in $(\mathcal{T})_{-1}$.

3. Exact deterministic solutions using the exp-function method

This section utilizes the exp-function method [30] alongside WN theory to derive a family of exact stochastic solutions for the (W-TS) geophysical KdV equation (1.1). By applying the HT to Eq (1.1), we obtain the corresponding deterministic equation:

$$\widetilde{Z}_\nu(\mu, \nu, w) + \widetilde{\Psi}(\nu, w)\widetilde{Z}_\mu(\mu, \nu, w) + \widetilde{\Phi}(\nu, w)\widetilde{Z}(\mu, \nu, w)\widetilde{Z}_\mu(\mu, \nu, w) + \widetilde{\Xi}(\nu, w)\widetilde{Z_{\mu\mu\mu}}(\mu, \nu, w) = 0, \tag{3.1}$$

where $w = (w_1, w_2, ...) \in (\mathbb{C}^{\mathbb{N}})_c$. To find traveling wave solutions for Eq (3.1), we introduce the following transformations:

$$\begin{cases} \widetilde{\Psi}(\nu, w) := \psi(\nu, w), \\ \widetilde{\Phi}(\nu, w) := \phi(\nu, w), \\ \widetilde{\Xi}(\nu, w) := \xi(\nu, w), \\ \widetilde{Z}(\mu, \nu, w) := z(\mu, \nu, w) = z(\chi(\mu, \nu, w)), \end{cases} \tag{3.2}$$

where

$$\chi(\mu, \nu, w) = \varsigma\mu + \lambda \int_0^{\nu} \vartheta(\tau, w) d\tau, \tag{3.3}$$

with ς and λ as arbitrary constants, and ϑ as a non-zero function to be determined. This transforms Eq (3.1) into the following NODE:

$$(\lambda\vartheta + \varsigma\psi + \varsigma\phi z) \frac{dz}{d\chi} + \varsigma^3 \xi \frac{d^3 z}{d\chi^3} = 0. \tag{3.4}$$

Using the exp-function method [30], the general solution of Eq (3.4) can be expressed as an expansion in terms of exponential functions:

$$z(\chi) = \frac{\sum_{n=-g}^{h} \eta_n(\nu, w) \exp(n\chi)}{\sum_{m=-i}^{j} \rho_m(\nu, w) \exp(m\chi)}, \tag{3.5}$$

where g, h, i, and j are freely chosen positive integers, and η_n and ρ_m are functions to be determined. Equation (3.5) may also be written in the form:

$$z(\chi) = \frac{\eta_g \exp(g\chi) + \ldots + \eta_{-h} \exp(-h\chi)}{\rho_i \exp(i\chi) + \ldots + \rho_{-j} \exp(-j\chi)}. \tag{3.6}$$

To determine appropriate values for g and i, we balance the highest-order linear term in Eq (3.4) with the highest-order nonlinear term. A straightforward computation gives:

$$\frac{d^3 z}{d\chi^3} = \frac{\epsilon_1 \exp[(7i + g)\chi] + \cdots}{\epsilon_2 \exp[8i\chi] + \cdots}, \tag{3.7}$$

and

$$z\frac{dz}{d\chi} = \frac{\epsilon_3 \exp[(i + 2g)\chi] + \cdots}{\epsilon_4 \exp[3i\chi] + \cdots} = \frac{\epsilon_3 \exp[(6i + 2g)\chi] + \cdots}{\epsilon_4 \exp[8i\chi] + \cdots}, \tag{3.8}$$

where ϵ_i are coefficients assigned solely for simplicity. By equating the highest-order term of the exponential function in Eqs (3.7) and (3.8), we obtain $7i + g = 6i + 2g$, which simplifies to $i = g$. Similarly, to find the values of h and j, we balance the lowest-order linear term in Eq (3.4):

$$\frac{d^3 z}{d\chi^3} = \frac{\cdots + \upsilon_1 \exp[-(7j + h)\chi]}{\cdots + \upsilon_2 \exp[-8j\chi]}, \tag{3.9}$$

with the term

$$z\frac{d^3z}{d\chi^3} = \frac{\cdots + \upsilon_3 \exp[-(j+2h)\chi]}{\cdots + \upsilon_4 \exp[-3j\chi]} = \frac{\cdots + \upsilon_3 \exp[-(6j+2h)\chi]}{\cdots + \upsilon_4 \exp[-8j\chi]}, \tag{3.10}$$

where υ_i are coefficients chosen only for simplicity. By equating the lowest-order term of the exponential function in Eqs (3.9) and (3.10), we obtain $-(7j+h) = -(6j+2h)$, which gives $j = h$. **Case 1.** Choosing $i = g = 1$ and $h = j = 1$, Eq (3.4) takes the form:

$$z(\chi) = \frac{\eta_1 \exp(\chi) + \eta_0 + \eta_{-1}\exp(-\chi)}{\rho_1 \exp(\chi) + \rho_0 + \rho_{-1}\exp(-\chi)}. \tag{3.11}$$

Substituting Eq (3.11) into Eq (3.4), and setting the coefficients of $\exp(\chi)$ to zero, results in a system of algebraic equations in η_0, η_1, η_{-1}, ρ_0, ρ_1, ρ_{-1}, and ϑ. Solving this system yields:

$$\begin{cases} \eta_1 = -\dfrac{\rho_0\left(6\varsigma^2\xi\rho_0 - \eta_0\phi\right)}{4\rho_{-1}\phi}, \quad \eta_{-1} = -\dfrac{\rho_{-1}\left(6\varsigma^2\xi\rho_0 - \eta_0\phi\right)}{\rho_0\phi}, \\ \rho_1 = \dfrac{\rho_0^2}{4\rho_{-1}}, \quad \vartheta = \dfrac{\varsigma\left(5\varsigma^3\xi\rho_0 - \eta_0\phi - \rho_0\psi\right)}{\lambda\rho_0}, \end{cases} \tag{3.12}$$

where η_0, ρ_0, and ρ_{-1} are free functions in $(\nu, w) \in \mathbb{R}_+ \times (\mathbb{C}^{\mathbb{N}})_c$.

By substituting the solutions from Eq (3.12) into Eq (3.11) and applying Eq (3.3), a soliton wave solution for Eq (3.1) can be obtained:

$$\begin{aligned} z_1(\mu,\nu,w) &= \Big[\left(\eta_0(\nu,w)\phi(\nu,w) - 6\varsigma^2\xi(\nu,w)\rho_0(\nu,w)\right)\left(\rho_0^2(\nu,w)A_{11}(\mu,\nu,w) + 4\rho_{-1}(\nu,w)A_{12}(\mu,\nu,w)\right) \\ &+ 4\rho_0(\nu,w)\rho_{-1}(\nu,w)\eta_0(\nu,w)\phi(\nu,w)\Big] \\ &\times \left[\rho_0(\nu,w)\phi(\nu,w)\left(\rho_0^2(\nu,w)A_{11}(\mu,\nu,w) + 4\rho_0(\nu,w)\rho_{-1}(\nu,w) + 4A_{12}(\mu,\nu,w)\right)\right]^{-1}, \end{aligned} \tag{3.13}$$

where

$$A_{11}(\mu,\nu,w) = \exp\left(\varsigma\mu + \varsigma\int_0^\nu \frac{5\varsigma^2\xi(\tau,w)\rho_0(\tau,w) - \eta_0(\tau,w)\phi(\tau,w) - \rho_0(\tau,w)\psi(\tau,w)}{\rho_0(\tau,w)}d\tau\right), \tag{3.14}$$

and

$$A_{12}(\mu,\nu,w) = \exp\left(-\left[\varsigma\mu + \varsigma\int_0^\nu \frac{5\varsigma^2\xi(\tau,w)\rho_0(\tau,w) - \eta_0(\tau,w)\phi(\tau,w) - \rho_0(\tau,w)\psi(\tau,w)}{\rho_0(\tau,w)}d\tau\right]\right). \tag{3.15}$$

Case 2. If we consider $i = g = 2$ and $j = h = 2$, the proposed solution in Eq (3.6) becomes:

$$z(\chi) = \frac{\eta_2\exp(2\chi) + \eta_1\exp(\chi) + \eta_0 + \eta_{-1}\exp(-\chi) + \eta_{-2}\exp(-2\chi)}{\rho_2\exp(2\chi) + \rho_1\exp(\chi) + \rho_0 + \rho_{-1}\exp(-\chi) + \rho_{-2}\exp(-2\chi)}. \tag{3.16}$$

To simplify the calculations, we set $\rho_1 = \rho_{-1} = 0$ and $\rho_2 = 0$. As a result, Eq (3.16) takes the form:

$$z(\chi) = \frac{\eta_2 \exp(2\chi) + \eta_1 \exp(\chi) + \eta_0 + \eta_{-1} \exp(-\chi) + \eta_{-2} \exp(-2\chi)}{\exp(2\chi) + \rho_0 + \rho_{-2} \exp(-2\chi)}. \tag{3.17}$$

Upon inserting Eq (3.17) into Eq (3.4), collecting the coefficients of $\exp(\chi)$, and equating them to zero, a system of algebraic equations is formed with variables $\eta_0, \eta_1, \eta_2, \eta_{-1}, \eta_{-2}, \rho_0, \rho_{-2}$, and ϑ. By solving this system with Mathematica, we find the following solutions:

$$\begin{cases} \eta_0 = \dfrac{\rho_0}{\phi}(12\varsigma^2\xi + \eta_2\phi), \quad \eta_1 = -\dfrac{6m\,\varsigma^2}{\phi}\left(\xi\sqrt{2\rho_0}\right), \quad \eta_{-1} = \dfrac{3m\,\varsigma^2}{\phi}\left(\xi\sqrt{2\rho_0^3}\right), \\ \eta_{-2} = \dfrac{1}{4}\eta_2^2\rho_0^2, \quad \rho_{-2} = \dfrac{1}{4}\rho_0^2, \quad \vartheta = -\dfrac{\varsigma}{\lambda}(\varsigma^2\xi + \eta_2\phi + \psi), \end{cases} \tag{3.18}$$

where ρ_0 and η_2 are arbitrary functions on $\mathbb{R}_+ \times (\mathbb{C}^{\mathbb{N}})_c$ and $m^2 = -1$.

Substituting the expressions from (3.18) into Eq (3.17) and applying Eq (3.3) leads to a soliton wave solution for Eq (3.1), presented below.

$$\begin{aligned} z_2(\mu,\nu,w) &= \Big[\phi(\nu,w)(4A_{23}(\mu,\nu,w) + \eta_2^2(\nu,w)\rho_0^2(\nu,w)A_{24}(\mu,\nu,w)) + 4\rho_0(\nu,w)(12\varsigma^2\xi(\nu,w) \\ &+ \eta_2(\nu,w)\phi(\nu,w)) + 12m\,\varsigma^2\xi(\nu,w)\sqrt{2\rho_0(\nu,w)}(\rho_0(\nu,w)A_{22}(\mu,\nu,w) - A_{21}(\mu,\nu,w))\Big] \\ &\times \left[4\phi(\nu,w)\left(A_{23}(\mu,\nu,w) + \rho_0(\nu,w) + \frac{1}{4}\rho_0^2(\nu,w)A_{24}(\mu,\nu,w)\right)\right]^{-1}, \end{aligned} \tag{3.19}$$

where

$$A_{21}(\mu,\nu,w) = \exp\left(\varsigma\mu - \varsigma\int_0^\nu \left(\varsigma^2\xi(\tau,w) + \eta_2(\tau,w)\phi(\tau,w) + \psi(\tau,w)\right)d\tau\right), \tag{3.20}$$

$$A_{22}(\mu,\nu,w) = \exp\left(-\left[\varsigma\mu - \varsigma\int_0^\nu \left(\varsigma^2\xi(\tau,w) + \eta_2(\tau,w)\phi(\tau,w) + \psi(\tau,w)\right)d\tau\right]\right), \tag{3.21}$$

$$A_{23}(\mu,\nu,w) = \exp\left(2\left[\varsigma\mu - \varsigma\int_0^\nu \left(\varsigma^2\xi(\tau,w) + \eta_2(\tau,w)\phi(\tau,w) + \psi(\tau,w)\right)d\tau\right]\right), \tag{3.22}$$

and

$$A_{24}(\mu,\nu,w) = \exp\left(-2\left[\varsigma\mu - \varsigma\int_0^\nu \left(\varsigma^2\xi(\tau,w) + \eta_2(\tau,w)\phi(\tau,w) + \psi(\tau,w)\right)d\tau\right]\right). \tag{3.23}$$

Case 3. If we set $i = g = 2$ and $j = h = 1$, then Eq (3.6) becomes:

$$z(\chi) = \frac{\eta_2 \exp(2\chi) + \eta_1 \exp(\chi) + \eta_0 + \eta_{-1} \exp(-\chi)}{\rho_2 \exp(2\chi) + \rho_1 \exp(\chi) + \rho_0 + \rho_{-1} \exp(-\chi)}. \tag{3.24}$$

To simplify the calculations, we set $\rho_2 = 1$. Using the procedures described above, we get:

$$\begin{cases} \eta_0 = \dfrac{\eta_2\rho_1^2}{3}, \quad \eta_1 = \eta_2\rho_1, \quad \eta_{-1} = \dfrac{\eta_2\rho_1^3}{27}, \\ \rho_0 = \dfrac{\rho_1^2}{3}, \quad \rho_{-1} = \dfrac{\rho_1^3}{27}, \quad \vartheta = \dfrac{-\xi\varsigma^3 - \eta_2\varsigma\phi - \varsigma\psi}{\lambda}, \end{cases} \tag{3.25}$$

where ρ_1 and η_2 are arbitrary functions on $\mathbb{R}_+ \times (\mathbb{C}^{\mathbb{N}})_c$.

Substituting the expressions from (3.25) into Eq (3.24) and applying Eq (3.3) leads to a soliton wave solution for Eq (3.1), presented below.

$$\begin{aligned} z_3(\mu,\nu,w) &= \Big[27\eta_2(\nu,w)A_{23}(\mu,\nu,w) + 27\eta_2(\nu,w)\rho_1(\nu,w)A_{21}(\mu,\nu,w) \\ &+ 9\eta_2(\nu,w)\rho_1^2(\nu,w) + \eta_2(\nu,w)\rho_1^3(\nu,w)A_{22}(\mu,\nu,w)\Big] \\ &\times \Big[27A_{32}(\mu,\nu,w) + 27\rho_1(\nu,w)A_{21}(\mu,\nu,w) + 9\rho_1^2(\nu,w) + \rho_1^3(\nu,w)A_{22}(\mu,\nu,w)\Big]^{-1}, \end{aligned} \tag{3.26}$$

where A_{21}, A_{22}, and A_{23} are defined in Eqs (3.24), (3.25), and (3.22), respectively.

Let ς be defined as an imaginary number. Under this assumption, the previously obtained soliton wave solutions can be converted into periodic forms. The corresponding transformations are:

$$\begin{cases} \varsigma = mB;\ B \in \mathbb{R} \text{ and } m^2 = -1, \\ e^{\pm m\chi} = \cos(\chi) \pm m\sin(\chi). \end{cases} \tag{3.27}$$

Consequently, the soliton solution presented in (3.13) is modified to:

$$\begin{aligned} z_4(\mu,\nu,w) &= \Big(\Big(\eta_0(\nu,w)\phi(\nu,w) + 6B^2\xi(\nu,w)\rho_0(\nu,w)\Big)\Big[\Big(\rho_0^2(\nu,w) + 4\rho_{-1}(\nu,w)\Big)\cos(BS(\mu,\nu,\tau)) \\ &+ m\Big(\rho_0^2(\nu,w) - 4\rho_{-1}(\nu,w)\Big)\sin(BS(\mu,\nu,\tau))\Big] + 4\rho_0(\nu,w)\rho_{-1}(\nu,w)\eta_0(\nu,w)\phi(\nu,w)\Big) \\ &\times \Big(\rho_0(\nu,w)\phi(\nu,w)\Big[\Big(\rho_0^2(\nu,w) + 4\rho_0(\nu,w)\rho_{-1}(\nu,w)\Big)\cos(BS(\mu,\nu,\tau)) \\ &+ m\Big(\rho_0^2(\nu,w) - 4\Big)\sin(BS(\mu,\nu,\tau))\Big]\Big)^{-1}, \end{aligned} \tag{3.28}$$

where

$$S(\mu,\nu,w) = \mu + \int_0^{\nu} \frac{5B^2\xi(\nu,w)\rho_0(\nu,w) - \eta_0(\nu,w)\phi(\nu,w) - \rho_0(\nu,w)\psi(\nu,w)}{\rho_0(\nu,w)} d\tau. \tag{3.29}$$

To achieve real periodic solutions, the imaginary component in Eq (3.28) must equal zero. To accomplish this, we assign the values $\rho_0(\nu,w) = \pm 2$ and $\rho_{-1}(\nu,w) = 1$. Consequently, we derive the following periodic solutions for Eq (3.1):

$$\begin{aligned} z_{41}(\mu,\nu,w) &= \frac{\eta_0(\nu,w)\phi(\nu,w) + 12B^2\xi(\nu,w)}{3\phi(\nu,w)} \\ &+ \frac{\eta_0}{3}\sec\left(B\left[\mu + \frac{1}{2}\int_0^{\nu}\Big(10B^2\xi(\tau,w) - \eta_0(\tau,w)\phi(\tau,w) - 2\psi(\tau,w)\Big)d\tau\right]\right), \end{aligned} \tag{3.30}$$

and

$$\begin{aligned} z_{42}(\mu,\nu,w) &= \frac{\eta_0(\nu,w)\phi(\nu,w) - 12B^2\xi(\nu,w)}{\phi(\nu,w)} \\ &- \eta_0\sec\left(B\left[\mu - \frac{1}{2}\int_0^{\nu}\Big(-10B^2\xi(\tau,w) - \eta_0(\tau,w)\phi(\tau,w) + 2\psi(\tau,w)\Big)d\tau\right]\right), \end{aligned} \tag{3.31}$$

Using the same approach as for the solution in Eq (3.13), the soliton wave solutions presented in (3.19) and (3.26) can be transformed into periodic wave solutions. Different parameter choices for i, g, h, and j enable the derivation of a variety of SPW solutions for Eq (3.1).

It is noteworthy that the construction of these soliton solutions imposes inherent relationships among the variable coefficients. These conditions ensure a balance between the linear and nonlinear terms, which is crucial for the existence of soliton structures. Similar intrinsic constraints have been reported in earlier works [35]. Although we do not impose explicit constraints beforehand, our method naturally satisfies these requirements.

4. Stochastic soliton and periodic wave solutions

The properties of exponential and trigonometric functions imply the existence of a bounded, open domain $\mathbb{O} \subset \mathbb{R}\times\mathbb{R}_+$, where the solution $z(\mu,\nu,w)$ to Eq (3.1) and all derivatives in Eq (3.1) are uniformly continuous for $(\mu,\nu,w) \in \mathbb{O}\times\mathcal{N}_\alpha(u)$, with $\alpha < \infty$ and $u > 0$. This solution remains continuous at each $(\mu,\nu) \in \mathbb{O}$ for any $w \in \mathcal{N}_\alpha(u)$ and is analytic in $w \in \mathcal{N}_\alpha(u)$ for fixed $(\mu,\nu) \in \mathbb{O}$. As stated in Theorem 2.1, there exists a stochastic distribution $Z(\mu,\nu) \in (\mathcal{T})_{-1}$, satisfying $z(\mu,\nu,w) = \widetilde{Z}(\mu,\nu)(w)$ for all $(\mu,\nu,w) \in \mathbb{O}\times\mathcal{N}_\alpha(u)$, and $Z(\mu,\nu)$ solves Eq (1.1) in $(\mathcal{T})_{-1}$. Consequently, applying the inverse HT to Eqs (3.13), (3.19), and (3.26) provides the exact soliton wave solutions for Eq (1.1) as follows:

$$\begin{aligned} Z_1(\mu,\nu) &= \Big[\Big(\eta_0^*(\nu)\diamond\Phi(\nu) - 6\varsigma^2\Xi(\nu)\diamond\rho_0^*(\nu)\Big)\diamond\Big((\rho_0^*)^{\diamond 2}(\nu)\diamond D_{11}(\mu,\nu) + 4\rho_{-1}^*(\nu)\diamond D_{12}(\mu,\nu)\Big) \\ &+ 4\rho_0^*(\nu)\diamond\rho_{-1}^*(\nu)\diamond\eta_0^*(\nu)\diamond\Phi(\nu)\Big] \\ &\diamond \Big[\rho_0^*(\nu)\diamond\Phi(\nu)\diamond\Big((\rho_0^*)^{\diamond 2}(\nu)\diamond D_{11}(\mu,\nu) + 4\rho_0^*(\nu)\diamond\rho_{-1}^*(\nu) + 4D_{12}(\mu,\nu)\Big)\Big]^{\diamond(-1)}, \end{aligned} \tag{4.1}$$

where

$$D_{11}(\mu,\nu) = \exp^\diamond\left(\varsigma\mu + \varsigma\int_0^\nu \frac{5\varsigma^2\Xi(\tau)\diamond\rho_0^*(\tau) - \eta_0^*(\tau)\diamond\Phi(\tau) - \rho_0^*(\tau)\diamond\Psi(\tau)}{\rho_0^*(\tau)}d\tau\right), \tag{4.2}$$

$$D_{12}(\mu,\nu) = \exp^\diamond\left(-\left[\varsigma\mu + \varsigma\int_0^\nu \frac{5\varsigma^2\Xi(\tau)\diamond\rho_0^*(\tau) - \eta_0^*(\tau)\diamond\Phi(\tau) - \rho_0^*(\tau)\diamond\Psi(\tau)}{\rho_0^*(\tau)}d\tau\right]\right), \tag{4.3}$$

and

$$\begin{aligned} Z_2(\mu,\nu) &= \Big[\Phi(\nu)\diamond(4D_{23}(\mu,\nu) + (\eta_2^*)^{\diamond 2}(\nu)\diamond(\rho_0^*)^{\diamond 2}(\nu)\diamond D_{24}(\mu,\nu)) + 4\rho_0^*(\nu)\diamond(12\varsigma^2\Xi(\nu) \\ &+ \eta_2^*(\nu)\diamond\Phi(\nu)) + 12m\,\varsigma^2\Xi(\nu)\diamond\sqrt{2\rho_0^*(\nu)}\diamond(\rho_0^*(\nu)\diamond D_{22}(\mu,\nu) - D_{21}(\mu,\nu))\Big] \\ &\diamond \Big[4\Phi(\nu)\diamond\Big(D_{23}(\mu,\nu) + \rho_0^*(\nu) + \frac{1}{4}(\rho_0^*)^{\diamond 2}(\nu)\diamond D_{24}(\mu,\nu)\Big)\Big]^{\diamond(-1)}, \end{aligned} \tag{4.4}$$

where

$$D_{21}(\mu,\nu) = \exp^\diamond\left(\varsigma\mu - \varsigma\int_0^\nu \Big(\varsigma^2\Xi(\tau) + \eta_2^*(\tau)\diamond\Phi(\tau) + \Psi(\tau)\Big)d\tau\right), \tag{4.5}$$

$$D_{22}(\mu,\nu)=\exp^{\diamond}\left(-\left[\varsigma\mu-\varsigma\int_0^{\nu}\left(\varsigma^2\Xi(\tau)+\eta_2^*(\tau)\diamond\Phi(\tau)+\Psi(\tau)\right)d\tau\right]\right), \tag{4.6}$$

$$D_{23}(\mu,\nu)=\exp^{\diamond}\left(2\left[\varsigma\mu-\varsigma\int_0^{\nu}\left(\varsigma^2\Xi(\tau)+\eta_2^*(\tau)\diamond\Phi(\tau)+\Psi(\tau)\right)d\tau\right]\right), \tag{4.7}$$

and

$$D_{24}(\mu,\nu)=\exp\left(-2\left[\varsigma\mu-\varsigma\int_0^{\nu}\left(\varsigma^2\Xi(\tau)+\eta_2^*(\tau)\diamond\Phi(\tau)+\Psi(\tau)\right)d\tau\right]\right), \tag{4.8}$$

$$\begin{aligned}Z_3(\mu,\nu) &= \left[27\eta_2^*(\nu)\diamond D_{23}(\mu,\nu)+27\eta_2^*(\nu)\diamond\rho_1^*(\nu)\diamond D_{21}(\mu,\nu)\right.\\ &+ \left.9\eta_2^*(\nu)\diamond(\rho_1^*)^{\diamond 2}(\nu)+\eta_2^*(\nu)\diamond(\rho_1^*)^{\diamond 3}(\nu)\diamond D_{22}(\mu,\nu)\right]\\ &\diamond \left[27D_{23}(\mu,\nu)+27\rho_1^*(\nu)\diamond D_{21}(\mu,\nu)+9(\rho_1^*)^{\diamond 2}(\nu)+(\rho_1^*)^{\diamond 3}(\nu)\diamond D_{22}(\mu,\nu)\right]^{\diamond(-1)},\end{aligned} \tag{4.9}$$

where D_{21}, D_{22}, and D_{23} are defined in Eqs (4.5), (4.6), and (4.7), respectively.

Also, by performing the inverse HT on Eqs (3.30) and (3.31), the exact periodic wave solutions for Eq (1.1) are obtained as follows:

$$\begin{aligned}Z_{41}(\mu,\nu) &= \frac{\eta_0^*(\nu)\diamond\Phi(\nu)+12B^2\diamond\Xi(\nu)}{3\Phi(\nu)}\\ &+ \frac{\eta_0^*}{3}\sec^{\diamond}\left(B\left[\mu+\frac{1}{2}\int_0^{\nu}\left(10B^2\Xi(\tau)-\eta_0^*(\tau)\diamond\Phi(\tau)-2\Psi(\tau)\right)d\tau\right]\right),\end{aligned} \tag{4.10}$$

and

$$\begin{aligned}Z_{42}(\mu,\nu) &= \frac{\eta_0^*(\nu)\diamond\Phi(\nu)-12B^2\Xi(\nu)}{\Phi(\nu)}\\ &- \eta_0^*\sec^{\diamond}\left(B\left[\mu-\frac{1}{2}\int_0^{\nu}\left(-10B^2\Xi(\tau)-\eta_0^*(\tau)\diamond\Phi(\tau)+2\Psi(\tau)\right)d\tau\right]\right).\end{aligned} \tag{4.11}$$

Here, $\rho_0^*, \rho_{-1}^*, \rho_1^*, \eta_0^*$, and η_2^* are arbitrary stochastic distributions in $(\mathcal{T})_{-1}$.

Moreover, the stochastic solutions derived in this work offer significant advantages in modeling real geophysical phenomena. For example, the inclusion of random perturbations allows the model to capture the complex variability observed in internal ocean waves and atmospheric gravity waves. This improved framework can more accurately represent the influence of environmental fluctuations on wave amplitude, energy distribution, and propagation dynamics, thereby enhancing its practical applicability in geophysical studies.

5. Illustrative example with numerical simulations

This section presents a specific example accompanied by numerical simulations to validate the significance of our findings and illustrate their practical applications. The solutions obtained for Eq (1.1) are significantly influenced by the configuration of the functions $\Phi(\nu)$, $\Psi(\nu)$, and $\Xi(\nu)$. Consequently, modifying the forms of these functions produces several solutions to Eq (1.1), as demonstrated in Eqs (4.1)–(4.11). This example demonstrates this behavior.

Example 5.1. *Consider the following setup: Let* $\Psi(\nu) = \delta_1\Phi(\nu)$, $\Xi(\nu) = \delta_2\Phi(\nu)$, $\Phi(\nu) = \varpi(\nu)+\delta_3\mathbb{W}(\nu)$, $\rho_0^*(\nu) = \delta_4$, $\rho_{-1}^* = \delta_5$, $\rho_1^* = \delta_6$, $\eta_0^* = \delta_7$, *and* $\eta_2^* = \delta_8$, *where the constants* $\delta_k\,(k = 1, 2, \ldots, 8)$ *are arbitrary,* $\varpi(\nu)$ *is a measurable function that is bounded on* $\mathbb{R}_+$, *and* $\mathbb{W}(\nu)$ *represents Gaussian WN, defined as the time derivative (in the strong sense within* $(\mathcal{T})_{-1}$*) of B-M* $\mathbb{B}(\nu)$. *The HT of* $\mathbb{W}(\nu)$ *is given by* $\widetilde{\mathbb{W}}(\nu, w) = \sum_{r=1}^{\infty} w_r \int_0^{\nu} \kappa_r(\tau)\, d\tau$ *[20]. Using the form of* $\widetilde{\mathbb{W}}(\nu, w)$, *Eqs* (4.1)–(4.11) *yield the WN functional solution for Eq* (1.1) *as follows:*

$$Z_{\mathbb{B}_1}(\mu,\nu) = \frac{(\delta_7 - 6\varsigma^2\delta_2)(\delta_4^2 \exp\left(\overline{D}_1(\mu,\nu)\right) + 4\delta_5 \exp\left(-\overline{D}_1(\mu,\nu)\right) + 4\delta_4\delta_5\delta_7}{\delta_4^3 \exp\left(\overline{D}_1(\mu,\nu)\right) + 4\delta_4\delta_5 + 4\exp\left(-\overline{D}_1(\mu,\nu)\right)}, \tag{5.1}$$

where

$$\overline{D}_1(\mu,\nu) = \varsigma\left[\mu + \frac{5\varsigma\delta_4\delta_2 - \delta_7 - \delta_4\delta_1}{\delta_4}\left[\int_0^{\nu} \varpi(\tau)d\tau + \delta_3\left(\mathbb{B}(\nu) - \frac{\nu^2}{2}\right)\right]\right], \tag{5.2}$$

$$\begin{aligned} Z_{\mathbb{B}_2}(\mu,\nu) &= \frac{1}{4\left(\exp\left(2\overline{D}_2(\mu,\nu)\right) + \delta_4 + \frac{1}{4}\delta_4^2\exp\left(-2\overline{D}_1(\mu,\nu)\right)\right)}\Big[4\exp\left(2\overline{D}_2(\mu,\nu)\right) \\ &+ \delta_8^2\delta_4^2\exp\left(-2\overline{D}_2(\mu,\nu)\right) + 4\delta_4(12\varsigma^2\delta_2 + \delta_8) + 12m\varsigma^2\delta_2\sqrt{2\delta_4}\Big(\delta_4\exp\left(-\overline{D}_2(\mu,\nu)\right) \\ &- \exp\left(\overline{D}_2(\mu,\nu)\right)\Big)\Big], \end{aligned} \tag{5.3}$$

where

$$\overline{D}_2(\mu,\nu) = \varsigma\left[\mu - (\varsigma^2\delta_2 + \delta_8 + \delta_1)\left[\int_0^{\nu} \varpi(\tau)d\tau + \delta_3\left(\mathbb{B}(\nu) - \frac{\nu^2}{2}\right)\right]\right], \tag{5.4}$$

$$Z_{\mathbb{B}_3}(\mu,\nu) = \frac{9\delta_8\left(3\exp\left(2\overline{D}_2(\mu,\nu)\right) + 3\delta_6\exp\left(\overline{D}_2(\mu,\nu)\right) + \delta_6^2\right) + \delta_8\delta_6^3\exp\left(-\overline{D}_2(\mu,\nu)\right)}{27\exp\left(2\overline{D}_2(\mu,\nu)\right) + 9\delta_6\left(3\exp\left(\overline{D}_2(\mu,\nu)\right) + \delta_6\right) + \delta_6^3\exp\left(-\overline{D}_2(\mu,\nu)\right)}, \tag{5.5}$$

where $\overline{D}_2$ *is defined in Eq* (5.4),

$$Z_{\mathbb{B}_4} = 4B^2\delta_2 + \frac{\delta_7}{3}\left\{1 + \sec\left(B\left(\mu + \frac{10B^2\delta_2 - \delta_7 - 2\delta_1}{2}\left[\int_0^{\nu} \varpi(\tau)d\tau + \delta_3\left(\mathbb{B}(\nu) - \frac{\nu^2}{2}\right)\right]\right)\right)\right\}, \tag{5.6}$$

and

$$Z_{\mathbb{B}_5} = 12B^2\delta_2 + \delta_7\left\{1 - \sec\left(B\left(\mu + \frac{10B^2\delta_2 + \delta_7 - 2\delta_1}{2}\left[\int_0^{\nu} \varpi(\tau)d\tau + \delta_3\left(\mathbb{B}(\nu) - \frac{\nu^2}{2}\right)\right]\right)\right)\right\}. \tag{5.7}$$

The numerical simulation of the soliton solution in (5.1) is shown in Figures 1 and 2, when $\delta_1 = 1$, $\delta_2 = 2$, $\delta_3 = 0.5$, $\delta_4 = 3$, $\delta_5 = 1.5$, $\delta_7 = 1.2$, $\varsigma = 0.7$, and $\varpi(\nu) = \tanh(2\nu)$. Figure 1 illustrates the behavior of the soliton solution (5.1) with stochastic influence, where the B-M $\mathbb{B}(\nu)$ is simulated as random noise with increments $d\mathbb{B} = \sqrt{\nu(2) - \nu(1)}$. RAND[0, 1]. Figure 2 represents the evolution of the the soliton solution (5.1) without stochastic influence, where the B-M $\mathbb{B}(\nu) = 0$. From Figures 1 and 2, it can be observed that the absence of B-M results in smooth, deterministic wave behavior. The inclusion of noise introduces stochastic fluctuations that influence the overall amplitude and structure of the soliton solution. Additionally, the stochastic forcing term in Figure 1 causes uncertainty in the wave amplitudes and disrupts the traveling wave patterns, leading to random variations in the soliton's behavior.

The numerical simulation of the periodic solution in (5.6) is shown in Figures 3 and 4, when $\delta_1 = 0.8$, $\delta_2 = 2$, $\delta_3 = 0.4$, $\delta_7 = 2$, and $B = 0.001$. The function $\varpi(\nu)$ is modified to exhibit stronger periodic behavior, defined as $\varpi(\nu) = \sin(2\pi\nu/\max(\nu)) + \cos(3\pi\nu/\max(\nu))$, contributing to the oscillations in the periodic solution (5.6). Figure 3 illustrates the periodic solution (5.6) with stochastic influence, where the B-M $\mathbb{B}(\nu)$ is simulated as amplified random noise with increments $d\mathbb{B} = \sqrt{\nu(2) - \nu(1)} \times 20 \cdot$ RAND[0, 1]. Figure 4 shows the behavior of the periodic solution (5.6) without stochastic influence, where $\mathbb{B}(\nu) = 0$. From Figures 3 and 4, we observe that the inclusion of B-M introduces significant stochastic fluctuations in the periodic solution. These fluctuations affect the overall amplitude and structure, leading to random variations in the system's behavior. The periodic function $\varpi(\nu)$ further amplifies the oscillations, creating a more complex wave pattern. In contrast, the absence of stochastic influence in Figure 4 results in smooth, deterministic wave behavior. The stochastic forcing term in Figure 3 creates uncertainty in the wave amplitudes, disrupting the periodic traveling wave patterns and leading to random distortions in the periodicity behavior.

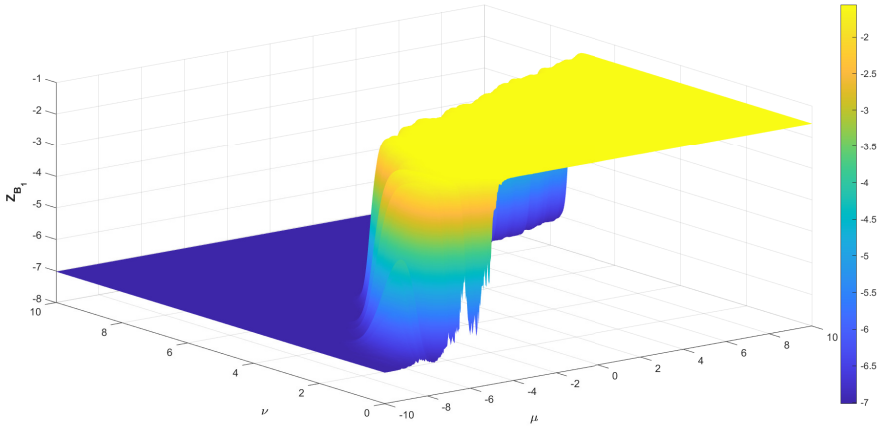

(a)

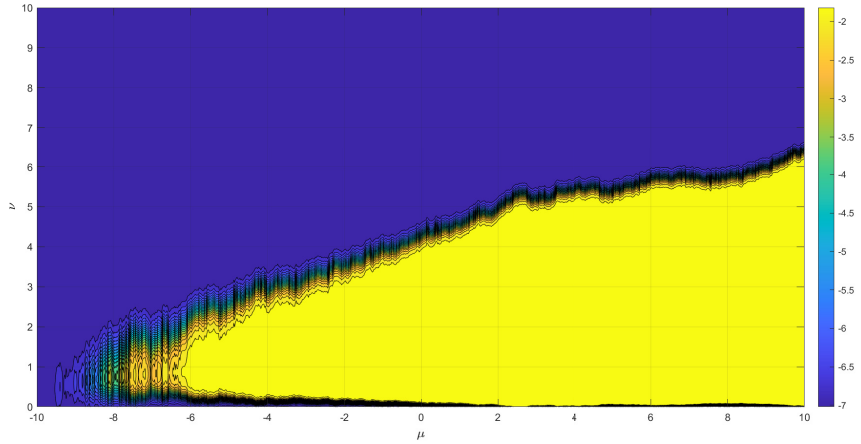

(b)

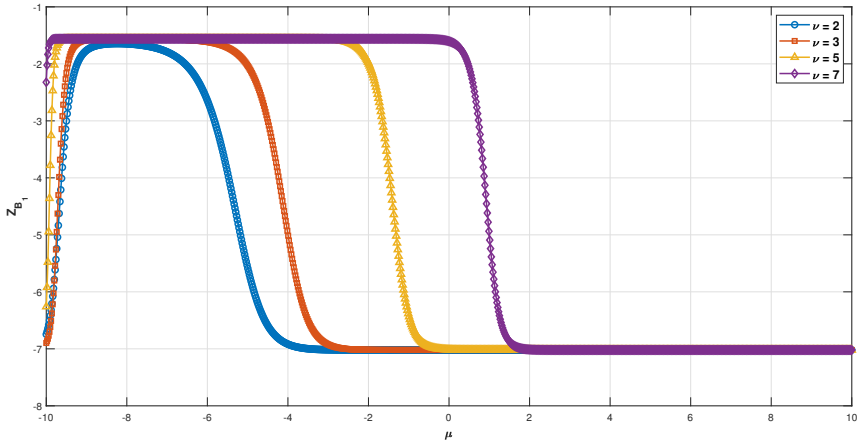

(c)

Figure 1. Visualization of the soliton solution in (5.1) including the effects of B-M: (a) 3D plot, (b) contour plot, and (c) 2D plot.

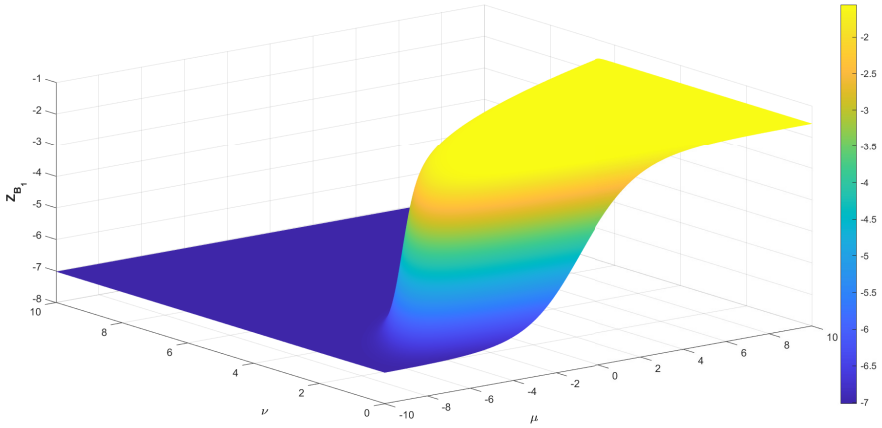

(a)

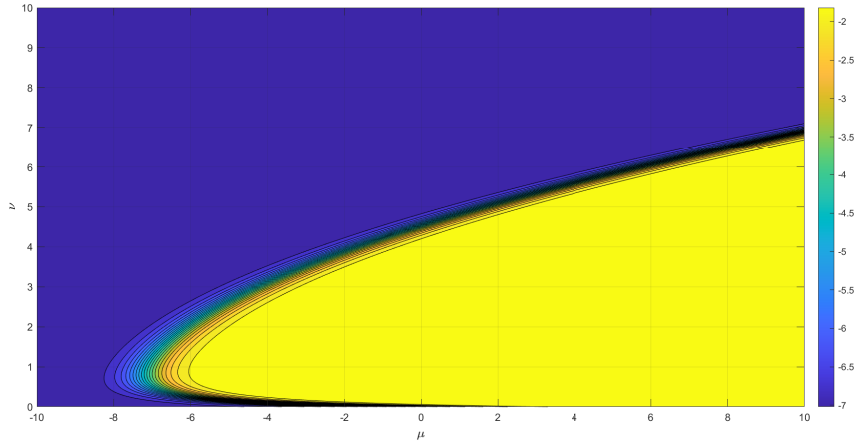

(b)

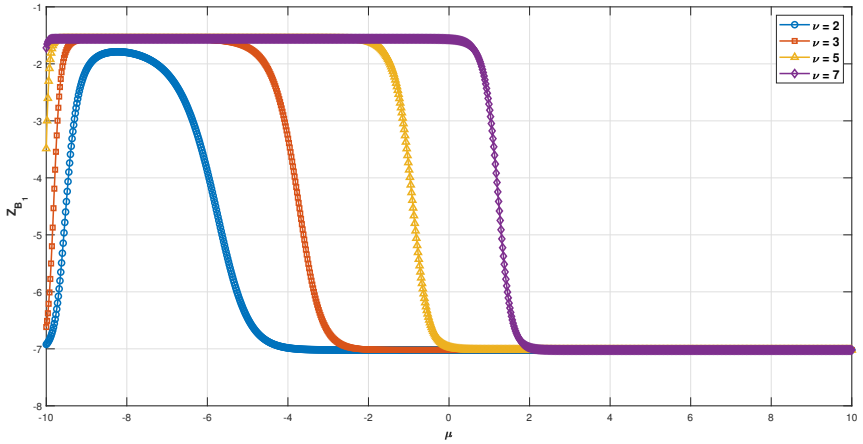

(c)

Figure 2. Visualization of the soliton solution in (5.1) excluding the effects of B-M: (a) 3D plot, (b) contour plot, and (c) 2D plot.

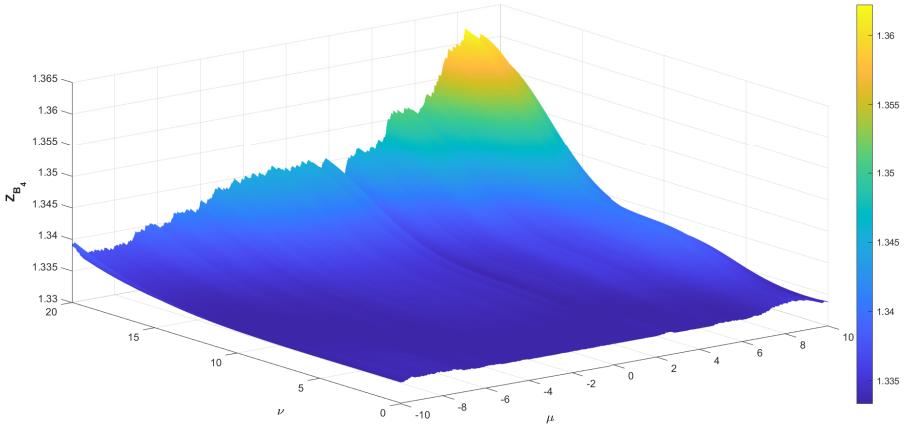

(a)

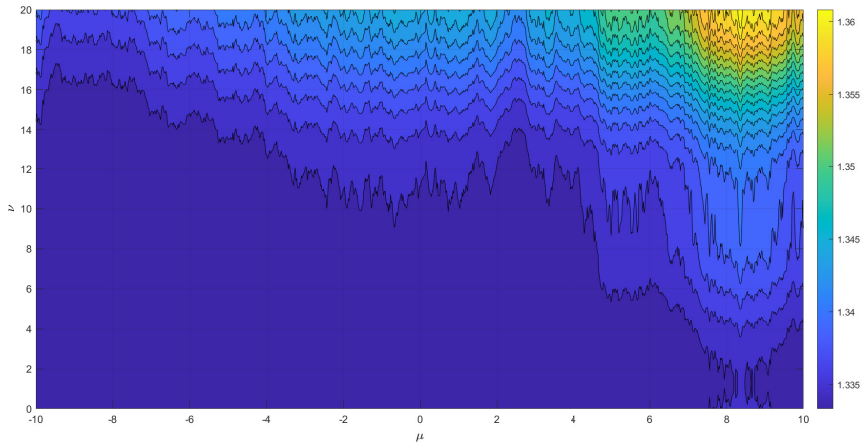

(b)

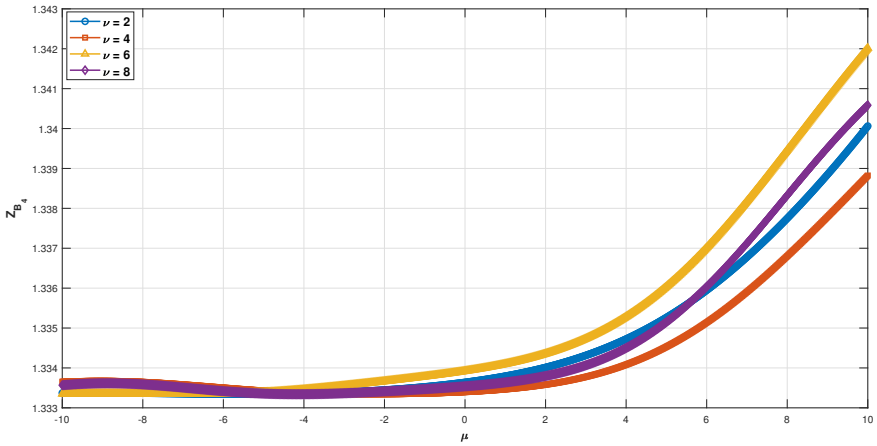

(c)

Figure 3. Visualization of the periodic solution in (5.6) with the effects of B-M: (a) 3D plot, (b) contour plot, and (c) 2D plot.

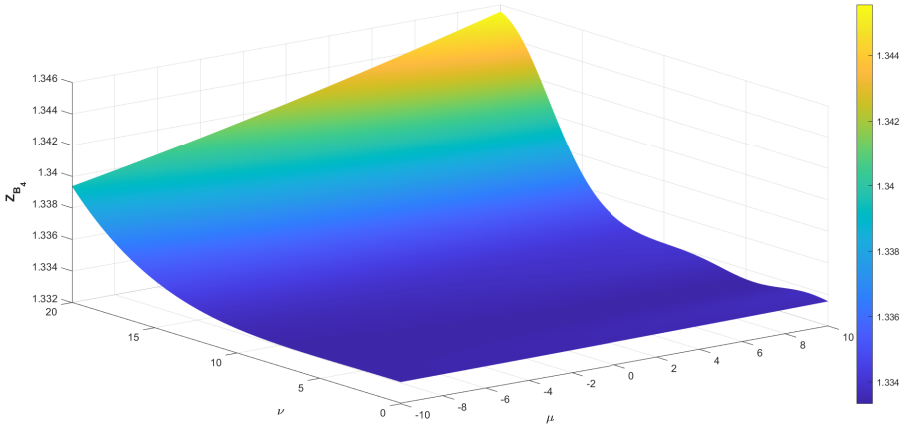

(a)

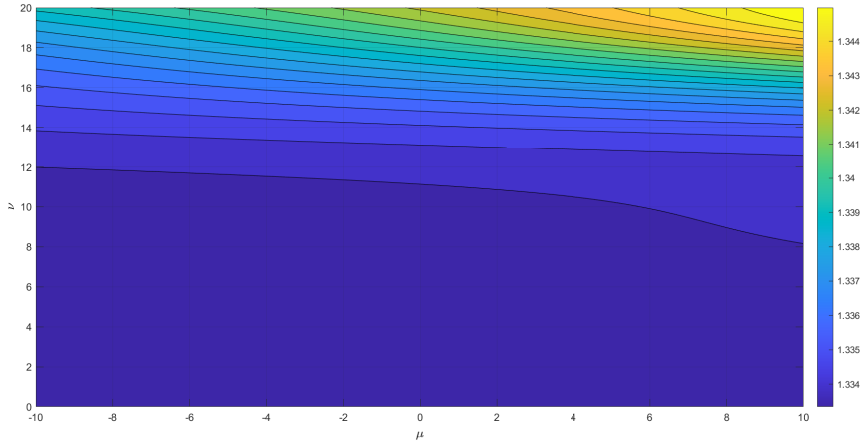

(b)

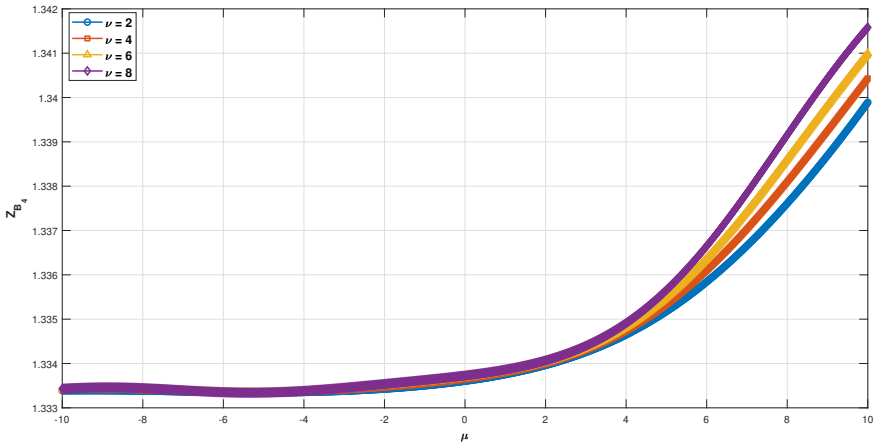

(c)

Figure 4. Visualization of the periodic solution in (5.6) without the effects of B-M: (a) 3D plot, (b) contour plot, and (c) 2D plot.

6. Conclusions

This research has derived precise SPW solutions for the stochastic geophysical KdV equation with variable coefficients, highlighting its importance for modeling wave phenomena in the atmosphere and oceans. By employing WN theory along with the HT, the stochastic equation was transformed into a deterministic form, enabling the application of the exp-function method. The solutions revealed that stochastic influences, such as B-M, introduce variability in wave forms, affecting both SPW dynamics. Numerical simulations demonstrated how these random fluctuations disrupt the smooth progression of waves, mirroring the complex dynamics observed in natural geophysical systems. The study offers a solid framework for exploring the interaction between deterministic and stochastic factors in large-scale wave propagation, providing valuable insights for future work on nonlinear wave equations with applications in fluid dynamics, oceanography, and atmospheric science. This study provides theoretical insights into geophysical wave dynamics that align with observed phenomena in the ocean and atmosphere. The deterministic solutions represent internal ocean waves and atmospheric gravity waves, both of which play crucial roles in energy transport and fluid mixing. The stochastic solutions incorporate environmental fluctuations such as wind stress variations and oceanic turbulence, which introduce uncertainties in wave behavior. Numerical simulations demonstrate how these perturbations influence wave stability and structure, reinforcing the real-world applicability of our findings. Future research could validate these results through experimental and observational studies in oceanography and atmospheric sciences.

Author contributions

Areej A. Almoneef, Abd-Allah Hyder, Mohamed A. Barakat, Abdelrheem M. Aly: Methodology, Conceptualization, Data curation, Writing-original draft, Investigation, Visualization, Validation, Writing-review and editing. All authors have read and approved the final version of the manuscript for publication.

Use of Generative-AI tools declaration

The authors declare they have not used Artificial Intelligence (AI) tools in the creation of this article.

Acknowledgments

The authors extend their appreciation to the Deanship of Research and Graduate Studies at King Khalid University for funding this work through the Research Groups Program under grant (RGP.2/82/45). The authors would like to acknowledge the Princess Nourah bint Abdulrahman University Researchers Supporting Project number (PNURSP2025R337).

Conflict of interest

The authors declare that there are no conflicts of interest regarding the publication of this article.

References

1. J. W. Miles, The Korteweg-de Vries equation: A historical essay, *J. Fluid Mech.*, **106** (1981), 131–147.
2. K. R. Khusnutdinova, Y. A. Stepanyants, M. R. Tranter, Soliton solutions to the fifth-order Korteweg-de Vries equation and their applications to surface and internal water waves, *Phys. Fluids*, **30** (2018), 022104. https://doi.org/10.1063/1.5009965
3. A. A. Hyder, A. H. Soliman, C. Cesarano, M. A. Barakat, Solving Schr$^{'}$odinger-Hirota equation in a stochastic environment and utilizing generalized derivatives of the conformable type, *Mathematics*, **9** (2021), 2760. https://doi.org/10.3390/math9212760
4. A. A. Hyder, M. A. Barakat, General improved Kudryashov method for exact solutions of nonlinear evolution equations in mathematical physics, *Phys. Scripta*, **95** (2020), 045212. https://doi.org/10.1088/1402-4896/ab6526
5. Attaullah, M. Shakeel, M. K. Alaoui, A. M. Zidan, N. A. Shah, Closed form solutions for the generalized fifth-order KDV equation by using the modified exp-function method, *J. Ocean Eng. Sci.*, In Press, 2022. https://doi.org/10.1016/j.joes.2022.06.037
6. K. R. Helfrich, W. K. Melville, Long nonlinear internal waves, *Ann. Rev. Fluid Mech.*, **38** (2006), 395–425. https://doi.org/10.1146/annurev.fluid.38.050304.092129
7. R. Grimshaw, E. Pelinovsky, T. Talipova, The modified Korteweg-de Vries equation in the theory of large-amplitude internal waves, *Nonlinear Proce. Geoph.*, **4** (1997), 237–250. https://doi.org/10.5194/npg-4-237-1997
8. S. T. R. Rizvi, A. R. Seadawy, F. Ashraf, M. Younis, H. Iqbal, D. Baleanu, Lump and interaction solutions of a geophysical Korteweg-de Vries equation, *Results Phys.*, **19** (2020), 103661. https://doi.org/10.1016/j.rinp.2020.103661
9. E. H. M. Zahran, A. Bekir, New unexpected behavior to the soliton arising from the geophysical Korteweg-de Vries equation, *Mod. Phys. Lett. B*, **36** (2022), 2150623. https://doi.org/10.1142/s0217984921506235
10. P. L. F. Liu, X. M. Wang, A multi-layer model for nonlinear internal wave propagation in shallow water, *J. Fluid Mech.*, **695** (2012), 341–365. https://doi.org/10.1017/jfm.2012.24
11. W. Hereman, Shallow water waves and solitary waves, *Solitons*, 2022, 203–220. https://doi.org/10.1007/978-1-0716-2457-9_480
12. Q. Li, Nonlinear internal waves in the South China Sea, *University of Rhode Island*, 2010. https://doi.org/10.23860/diss-2353
13. J. P. Boyd, *Nonlinear equatorial waves*, Dynamics of the equatorial ocean, Heidelberg: Springer, 2017, 329–404. https://doi.org/10.1007/978-3-662-55476-0_16
14. H. F. Ismael, M. A. S. Murad, H. Bulut, Various exact wave solutions for KdV equation with time-variable coefficients, *J. Ocean Eng. Sci.*, **7** (2022), 409–418. https://doi.org/10.1016/j.joes.2021.09.014

15. A. K. Gupta, S. S. Ray, On the solution of time-fractional KdV-Burgers equation using Petrov-Galerkin method for propagation of long wave in shallow water, *Chaos, Soliton. Fract.*, **116** (2018), 376–380. https://doi.org/10.1016/j.chaos.2018.09.046

16. R. Grimshaw, *Environmental stratified flows*, Springer Science & Business Media, 2002. https://doi.org/10.1007/b100815

17. A. R. Osborne, *Nonlinear ocean wave and the inverse scattering transform*, Scattering, 2002, 637–666. https://doi.org/10.1016/b978-012613760-6/50033-4

18. D. Kaya, Partial differential equations that lead to solitons, *Solitons*, 2022, 193–201. https://doi.org/10.1007/978-1-0716-2457-9_380

19. A. Geyer, R. Quirchmayr, Shallow water equations for equatorial tsunami waves, *Philos. T. Roy. Soc. A: Math. Phys. Eng. Sci.*, **376** (2018), 20170100. https://doi.org/10.1098/rsta.2017.0100

20. H. Holden, B. Øksendal, J. Ubøe, T. Zhang, *Stochastic partial differential equations*, Springer, 2010. https://doi.org/10.1007/978-0-387-89488-1_5

21. H. Yépez-Martínez, J. F. Gómez-Aguilar, D. Baleanu, Beta-derivative and sub-equation method applied to the optical solitons in medium with parabolic law nonlinearity and higher order dispersion, *Optik*, **155** (2018), 357–365. https://doi.org/10.1016/j.ijleo.2017.10.104

22. H. M. Baskonus, J. F. Gómez-Aguilar, New singular soliton solutions to the longitudinal wave equation in a magneto-electro-elastic circular rod with M-derivative, *Mod. Phys. Lett. B*, **33** (2019), 1950251. https://doi.org/10.1142/s0217984919502518

23. B. Ghanbari, J. F. Gómez-Aguilar, Optical soliton solutions for the nonlinear Radhakrishnan-Kundu-Lakshmanan equation, *Mod. Phys. Lett. B*, **33** (2019), 1950402. https://doi.org/10.1142/s0217984919504025

24. C. Qian, J. G. Rao, Y. B. Liu, J. S. He, Rogue waves in the three-dimensional Kadomtsev-Petviashvili equation, *Chinese Phys. Lett.*, **33** (2016), 110201. https://doi.org/10.1088/0256-307x/33/11/110201

25. X. R. Hu, J. C. Chen, Y. Chen, Groups analysis and localized solutions of the (2+1)-dimensional Ito equation, *Chinese Phys. Lett.*, **32** (2015), 070201. https://doi.org/10.1088/0256-307x/32/7/070201

26. X. Z. Liu, J. Yu, Z. M. Lou, X. M. Qian, A nonlocal Burgers equation in atmospheric dynamical system and its exact solutions, *Chinese Phys. B*, **28** (2019), 010201. https://doi.org/10.1088/1674-1056/28/1/010201

27. P. F. Zheng, M. Jia, A more general form of lump solution, lumpoff, and instanton/rogue wave solutions of a reduced (3+1)-dimensional nonlinear evolution equation, *Chinese Phys. B*, **27** (2018), 120201. https://doi.org/10.1088/1674-1056/27/12/120201

28. S. Q. Xu, X. G. Geng, N-soliton solutions for the nonlocal two-wave interaction system via the Riemann-Hilbert method, *Chinese Phys. B*, **27** (2018), 120202. https://doi.org/10.1088/1674-1056/27/12/120202

29. X. Y. Jiao, Truncated series solutions to the (2+1)-dimensional perturbed Boussinesq equation by using the approximate symmetry method, *Chinese Phys. B*, **27** (2018), 100202. https://doi.org/10.1088/1674-1056/27/10/100202

30. J. H. He, X. H. Wu, Exp-function method for nonlinear wave equations, *Chaos, Soliton. Fract.*, **30** (2006), 700–708. https://doi.org/10.1016/j.chaos.2006.03.020

31. N. A. Kudryashov, N. B. Loguinova, Be careful with the exp-function method, *Commun. Nonlinear Sci. Numer. Simul.*, **14** (2009), 1881–1890. https://doi.org/10.1016/j.cnsns.2008.07.021 .

32. N. A. Shah, Y. S. Hamed, K. M. Abualnaja, J. D. Chung, R. Shah, A. Khan, A Comparative analysis of fractional-order Kaup-Kupershmidt equation within different operators, *Symmetry*, **14** (2022), 986. https://doi.org/10.3390/sym14050986

33. M. Shakeel, Attaullah, N. A. Shah, J. D. Chung, Application of modified exp-function method for strain wave equation for finding analytical solutions, *Ain Shams Eng. J.*, **14** (2023), 101883. https://doi.org/10.1016/j.asej.2022.101883

34. S. Zhang, Exact solutions of Wick-type stochastic KdV equation, *Can. J. Phys.*, **90** (2012), 181–186. https://doi.org/10.1139/p2012-002

35. S. Zhang, H. W. Li, B. Xu, Inverse scattering integrability and fractional soliton solutions of a variable-coefficient fractional-order KdV-type equation, *Fractal Fract.*, **8** (2024), 520. https://doi.org/10.3390/fractalfract8090520

AIMS Press